

Comparison of the performance of photonic band-edge liquid crystal lasers using different dyes as the gain medium

Carrie Mowatt,^{1,a)} Stephen M. Morris,¹ Myoung Hoon Song,^{2,b)} Timothy D. Wilkinson,¹ Richard H. Friend,² and Harry J. Coles^{1,c)}

¹Centre of Molecular Materials for Photonic and Electronics, Electrical Engineering Division, Department of Engineering, University of Cambridge, 9 JJ Thomson Avenue, Cambridge CB3 0FA, United Kingdom

²Cavendish Laboratory, University of Cambridge, Cambridge CB3 0HE, United Kingdom

(Received 4 September 2009; accepted 6 December 2009; published online 16 February 2010)

The primary concern of this work is to study the emission characteristics of a series of chiral nematic liquid crystal lasers doped with different laser dyes (DCM, pyromethene 580, and pyromethene 597) at varying concentrations by weight (0.5–2 wt %) when optically pumped at 532 nm. Long-wavelength photonic band-edge laser emission is characterized in terms of threshold energy and slope efficiency. At every dye concentration investigated, the pyromethene 597-doped lasers exhibit the highest slope efficiency (ranging from 15% to 32%) and the DCM-doped lasers the lowest (ranging from 5% to 13%). Similarly, the threshold was found to be, in general, higher for the DCM-doped laser samples in comparison to the pyromethene-doped laser samples. These results are then compared with the spectral properties, quantum efficiencies and, where possible, fluorescence lifetimes of the dyes dispersed in a common nematic host. In accordance with the low thresholds and high slope efficiencies, the results show that the molar extinction coefficients and quantum efficiencies are considerably larger for the pyromethene dyes in comparison to DCM, when dispersed in the liquid crystal host. © 2010 American Institute of Physics. [doi:10.1063/1.3284939]

I. INTRODUCTION

Recent progress in soft-matter photonic band structures has highlighted dye-doped chiral nematic liquid crystals (N*LCs) as a new class of organic laser device. Lasers of this type retain the tunability of a liquid dye laser while allowing for the design of compact and self-contained laser systems. Furthermore, these liquid crystal (LC) lasers avoid the use of the toxic and volatile solvents that are often used in conventional “jet stream” dye lasers. N*LCs have the added benefit that they are self-organizing organic structures that form left or right handed helices which repeat over a distance known as the pitch, p .¹ Under certain experimental conditions, the periodicity gives rise to a one dimensional photonic band-gap (PBG) for circularly polarized light with the same sense of rotation as the helix. The presence of a PBG suppresses spontaneous emission of photons within the gap² and enhances it at the edges.³ When a laser dye is dispersed in the N*LC matrix, the enhancement of emission at the band edges can be sufficient to enable low threshold laser action.⁴ For more details on the laser mechanism, see Ref. 5. Further, the periodicity of the helix can be altered using external stimuli (e.g., temperature control and electric fields), enabling the

emission wavelength to be tuned. As a result, N*LC lasers offer an attractive alternative to lasers based on semiconductor technology.

For these tunable microlasers to be incorporated into a wide range of practical applications, it is important that their excitation thresholds must be reduced and their efficiencies increased. As a starting point, these characteristics can be improved through optimization of the materials from which the devices are constructed. Studies using one laser dye (DCM, see Fig. 1) in a variety of liquid crystalline hosts have

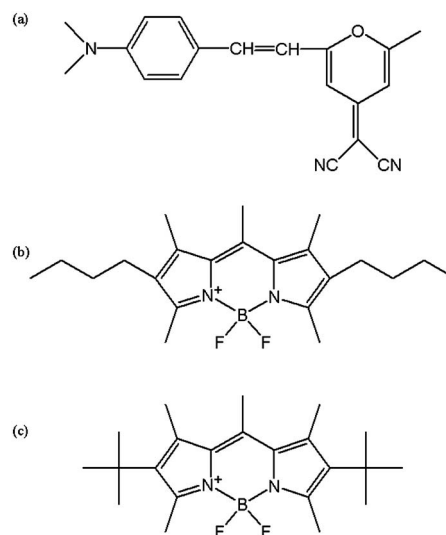


FIG. 1. Chemical structures of the laser dyes used in this study: (a) DCM, (b) pyromethene 580 (PM580), and (c) pyromethene 597 (PM597).

^{a)}Electronic mail: cg323@cam.ac.uk.

^{b)}Present address: School of Mechanical and Advanced Materials Engineering, Ulsan National Institute of Science and Technology (UNIST), Ulsan, South Korea.

^{c)}Author to whom correspondence should be addressed. Electronic mail: hjc37@cam.ac.uk.

shown that the emission properties of dye-doped N*LC lasers are related to the physical properties of the host. High values of the birefringence, Δn ,⁶⁻⁹ the orientational order parameter S_2 ,⁸⁻¹⁰ and the elastic properties⁹ have been found to correlate with low thresholds and high slope efficiencies.^{8,9}

Macroscopic properties, such as the birefringence and order parameter, relate to the resonatorlike structure of the chiral nematic phase. The emissive attributes, on the other hand, are determined by the gain medium which is dissolved in the LC. In general, the emission intensity of a dye dissolved in a solvent depends on factors such as the absorption and emission cross sections, the fluorescence lifetime, and the quantum efficiency. In addition, when laser dyes are dissolved in the LC media, the orientation of the dye molecules with respect to the “local” director must be taken into account. The impact of the dye ordering on the spontaneous emission rate has been treated theoretically and experimentally by Schmidtke and Stille.¹¹ Using Fermi’s golden rule, it was shown that the spontaneous emission rate has a dependence on the orientational order parameter of the dye transition dipole moment, S_T . There is also evidence to suggest that S_T affects the stimulated emission rate as well^{7,8,11} and, as a result, correlations have been found linking high order parameters with low excitation thresholds of the corresponding LC laser.

Laser dyes, in general, have attracted considerable attention recently because of their connection with possible applications such as visualizing agents in biological systems, organic light emitting diodes, and solar energy concentrators. As a result, research has been conducted on determining the photophysical properties of these dyes in polymer hosts in comparison to isotropic liquid solvents.^{12,13} It has been found that to a large extent, the photophysical and photochemical processes are determined by the polarity of the solvent. Generally, the emission of the dye is a result of intramolecular charge transfer between electron-donating and electron-accepting units. Intermolecular interactions with the host can cause the emission efficiency to increase or decrease depending on whether highly efficient states are stabilized or non-radiative pathways are favored.

Two of the most widely used dyes for LC lasers that have been studied thus far are DCM and PM597, Fig. 1. DCM is a prime example of an electron donor/acceptor compound, which results from intramolecular charge transfer between the electron-donating (dimethylamino group) and electron-accepting (pyran ring with two cyano groups) units. Consequently, the emissive attributes of the dye can vary greatly depending on the host. In the context of LC lasers, properties such as quantum efficiency and fluorescence lifetimes of laser dyes dispersed in a LC host are likely to differ from conventional solvents, and this will have an impact on the thresholds and efficiencies of the corresponding lasers. The difference in thresholds and efficiencies for LC lasers using different laser dyes and the connection with the photophysical properties such as quantum efficiency and lifetime has not, as yet, been studied in detail.

The purpose of this study was to investigate how the threshold energy for lasing and the slope efficiency (defined as the rate of change of output energy/input energy above the

lasing threshold) vary when different dyes are dispersed in a common LC host. We have quantitatively compared band-edge laser emission from three different laser dyes: DCM, pyrromethene 580 (PM580), and pyrromethene 597 (PM597), when optically pumped at $\lambda=532$ nm. Our results show that, for a given liquid crystalline host, the laser threshold energy and slope efficiency can vary dramatically depending on the dye and concentration thereof. For example, the slope efficiency is found to range from 15% to 32% for PM597-doped LC lasers, depending on the dye concentration. In addition to the input-output characteristics of the lasers, results are presented for molar extinction coefficients, quantum efficiencies, and, in some cases, fluorescence lifetimes of the laser dyes when dispersed in the LC host. Finally, we consider and discuss the connection between the photophysical properties and the performance characteristics of the LC lasers to gain an insight as to the physical reasoning behind the different results.

This paper is organized as follows: preparation of the mixtures for spectroscopic and laser studies, and the experimental procedure used to acquire results are discussed in Secs. II and III, respectively. Following this, the results obtained for the photophysical properties of the dye and the emission characteristics of the different lasers are presented in Sec. IV, the discussion of the results is provided in Sec. V, and finally concluding remarks are made in Sec. VI.

II. SAMPLE PREPARATION

A. Laser dyes

The three laser dyes chosen as gain media were 4-dicyanimethylene-2-methyl-6-(p-dimethylaminostyryl)-4H-pyran (DCM, Lambda Physik), 4,4-difluoro-2,6-di-n-butyl-1,3,5,7,8-pentamethylpyrromethenedifluoroborate complex (pyrromethene 580, Exciton), and 4,4-difluoro-2,6-di-t-butyl-1,3,5,7,8-pentamethylpyrromethenedifluoroborate complex (pyrromethene 597, Exciton). These dyes were used as received, without further purification. These dyes were chosen for the following reasons: they are all known to be soluble in LC media. DCM has a broad fluorescence wavelength range, thus is widely used in laser spectroscopy. Furthermore, it is the most studied dye in LC lasers. The pyrromethene dyes have a narrower emission range but are known to be highly efficient emitters. Their efficiency is attributed to their planar structure and low triplet-triplet absorption, leading to high fluorescence yields.¹⁴

The chemical structures of the dyes are shown in Fig. 1. The pyrromethene dyes are structural isomers and so have identical molecular weights (374.32 amu). However, DCM has a different molecular weight (303.36 amu). Consequently, at each percentage by weight of dye, the ground state populations of the DCM and pyrromethene based systems are slightly different. However, this is not expected to significantly affect our results and conclusions. The dyes were dissolved in the LC following the methods described below.

B. Nematic LC

For the LC, a single eutectic nematic host (E49, Merck NB-C) was used throughout this study. E49 is a well-known commercial nematogenic mixture consisting of cyano-biphenyls and terphenyls. This host was chosen because it has relatively high values of birefringence, Δn , and orientational order parameter, S_2 , the main physical properties required for efficient low threshold photonic band-edge (PBE) lasing⁷⁻¹⁰ (for E49, $\Delta n=0.25$ and $S_2=0.66$ at 30 °C) and is liquid crystalline at room temperature. For absorbance and spontaneous emission measurements, solutions containing E49 and various concentrations of each laser dye were used.

C. Chiral nematic LC

Chiral nematic mesophases were induced via the addition of a chiral dopant to the dye-doped nematic solutions. The high twisting power (helical twisting power $\approx 0.7 \mu\text{m}^{-1}$ in E49) chiral dopant known as BDH1281 (Merck NB-C) was selected because only a relatively small percentage of this material ($\sim 3-5$ wt %) is required to induce a PBG in the visible wavelength range. The concentration of chiral dopant for each dye-E49 combination was selected such that the long-wavelength PBE corresponded to the emission wavelength which exhibited maximum efficiency (λ_{opt} , described in Sec. IV E).

The dyes and chiral dopant were initially dissolved by heating with a localized heat source and agitating the mixture. To ensure that the solutes had fully dissolved, each mixture was then heated into the isotropic phase (approximately 10 °C above the clearing temperature) in a bake oven for up to 9 h. The resulting solutions were found to be free from dye crystals over the entire chiral nematic phase range when examined under a microscope. Solutions in the isotropic phase were then capillary filled into cells (Merck NB-C) with rubbed polyimide alignment layers. This resulted in a planar texture (director parallel to the glass substrates) for dye-doped nematic samples and a Grandjean texture (helix axis perpendicular to the substrates) for dye-doped chiral nematic samples. When examined by polarizing optical microscopy, the Grandjean textures were found to consist of large monodomains (>1 mm across) almost entirely free from oily streak disclinations. A previous study has shown that monodomains are important for single-mode laser emission.¹⁵

III. EXPERIMENTAL PROCEDURE

For measurements requiring laser excitation, such as spontaneous emission (fluorescence) and PBE laser emission, a frequency doubled Q-switched neodymium-doped yttrium aluminum garnet (Nd:YAG) laser ($\lambda=532$ nm, Nano T, Litron) was used to excite the samples. This typically results in an electronic transition to the first excited state e.g., S_0 to S_1 . The repetition rate and pulse length were 1 Hz and ≈ 6 ns, respectively. This repetition rate was selected in order to minimize the undesired effects of optical reorientation¹⁶ and sample heating. For all emission measurements, the cell thickness was kept constant at 10 μm . For spontaneous emission measurements, linearly polarized light was used to

excite the sample, whereas for laser emission measurements, a quarter-wave Fresnel rhomb was used to convert the incident polarization from linearly to circularly polarized with the opposite sense of rotation to that of the sample helix. The purpose of the Fresnel rhomb was to maximize the penetration depth of the pump light. A lens ($f=10$ cm) was used to focus the pump beam to a spot of $\approx 160 \mu\text{m}$ diameter at the sample. The samples were mounted on a temperature controlled heating stage (Linkam stage with TP91 controller). The emission from the samples was collected in the forward direction (perpendicular to the cell walls) using a series of collection optics. For spectral measurements, a universal serial bus (USB) spectrometer was used (resolution=0.3 nm, HR2000, Ocean Optics), whereas emission energy measurements were made using an energy meter (PD10 silicon photodiode head with Laserstar energy meter, Ophir).

Absorption and transmission measurements were made using the HR2000 spectrometer attached to a polarizing microscope (Olympus BH-2, analyzer removed) via collection optics and an optical fiber (200 μm diameter core). The absorbance spectra of each dye-doped nematic sample were measured using white light polarized parallel and perpendicular to the director (denoted A_{\parallel} and A_{\perp} , respectively). For each sample, the cell thickness was selected to give a strong A_{\parallel} signal without saturation. Clearing temperatures, T_c , were also measured using the polarizing microscope. For this study, T_c was taken to be the temperature at which the nematic phase (indicated by a Schlieren texture¹⁷) first began to appear upon cooling from the isotropic phase at a rate of 5 °C/min. All other measurements were made at a temperature of 30 ± 1 °C.

The photoluminescence efficiency was determined for the three dyes for four different concentrations, using an experimental technique described elsewhere.¹⁸ The experimental setup consisted fundamentally of an argon-ion laser as the excitation source and an integrating sphere with which to collect the emission from the sample. Samples were confined between circular quartz cells and were mounted within the integrating sphere. The excitation wavelengths were 475 nm for the DCM samples and 514 nm for the pyromethene samples. The fluorescence lifetimes were determined for DCM in the nematic LC host using a time correlated single photon counting method. The DCM samples were optically excited at 475 nm.

IV. RESULTS

A. Spectral properties

Figure 2 shows the steady-state absorbance spectrum (for white light) and the corresponding unsaturated fluorescence spectrum (when optically excited at $\lambda=532$ nm) for 1 wt % of each dye in E49. In both cases, the incident light was polarized parallel to the director. The spontaneous emission spectra have been normalized for comparison, such that the maximum value is unity, since different excitation energies were used for each sample. The peak wavelengths of both absorption and spontaneous emission were found to be approximately independent of concentration for all three dyes. The peak absorption wavelengths were at 530 and 526

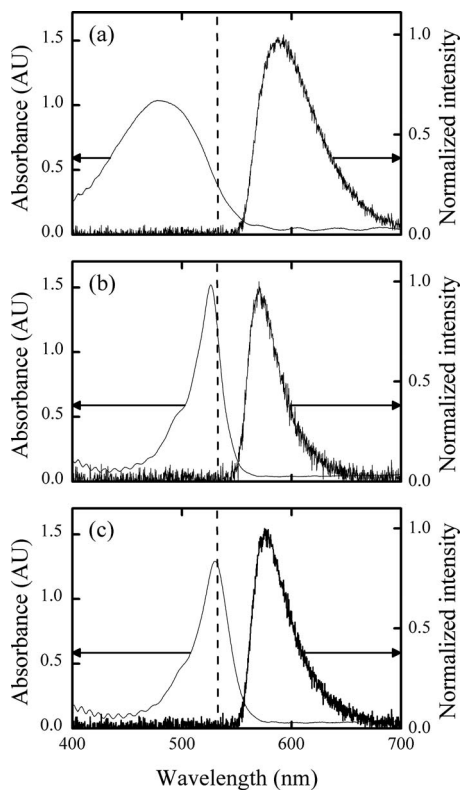


FIG. 2. Examples of absorbance and unsaturated spontaneous emission (fluorescence) spectra parallel to the director for the dye-doped nematic samples (1 wt % dye in E49): (a) DCM (b) PM580, and (c) PM597. The pump wavelength, 532 nm, is indicated by the dashed lines on the absorbance spectra. The spontaneous emission spectra have been normalized such that the maximum value is 1, because different excitation energies were used for each sample.

nm for PM597 and PM580, respectively, with full widths at half maximum (FWHMs) of ~ 34 nm. In contrast, the absorption peak of DCM was at the much shorter wavelength of 479 nm, with a much broader FWHM of 97 nm. Clearly, the absorbance peaks of the pyrromethene dyes are closer to the pump wavelength (532 nm, indicated by the dashed lines in Fig. 2) than that of DCM. The fluorescence peaks, on the other hand, were found to be at 589, 571, and 577, for DCM, PM580, and PM597, respectively. The broad fluorescence of DCM (FWHM=60 nm) makes it particularly useful for wavelength tuning applications. It is also apparent that the Stokes shift of DCM (110 nm) is considerably larger than that of the pyrromethene dyes (45 nm). The absence of structure in the fluorescence bands is indicative of dyes with intramolecular charge transfer in a polar solvent.¹⁹

B. Molar extinction coefficients

To determine the molar extinction coefficients of the different solutions, the absorbance at the pump wavelength has been measured for each dye dissolved in the achiral nematic LC host. The absorbance parallel to the helical axis of a N*LC sample is given by

$$\bar{A} = \sqrt{\frac{1}{2}(A_{\parallel}^2 + A_{\perp}^2)}, \quad (1)$$

where A_{\parallel} is the absorbance parallel to the “local” director and A_{\perp} is the absorbance perpendicular to the “local” director.

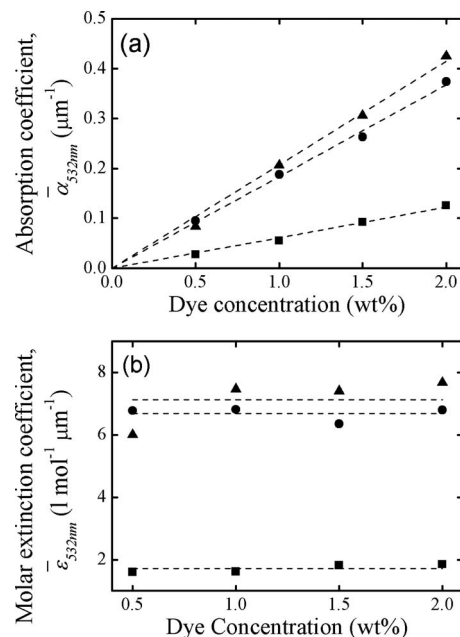


FIG. 3. The absorption properties of the dye-doped samples. (a) The absorption coefficient as a function of dye concentration, where the dashed lines indicate a linear dependence on concentration. (b) The molar extinction coefficient as a function of dye concentration, where the dashed lines indicate that the extinction coefficient is approximately independent of dye concentration. The key for the figure is as follows: DCM (■), PM580 (●), and PM597 (▲).

From herein, the absorbance parallel to the helix axis is referred to as the mean absorbance, \bar{A} . The molar extinction is related to the absorbance through the Beer–Lambert law, i.e., $A = \alpha d = \epsilon c d$, where α and ϵ are the absorption and molar extinction coefficients, respectively, c is the concentration, and d is the sample thickness.

The mean absorption and molar extinction coefficients for the three dyes at the pump wavelength ($\lambda = 532$ nm) are plotted as a function of the dye concentration in Fig. 3. The order, in increasing magnitudes of $\bar{\alpha}_{532 \text{ nm}}$ and $\bar{\epsilon}_{532 \text{ nm}}$, was found to be DCM, PM580, and PM597. The dashed lines in Fig. 3(a) indicate that $\alpha_{532 \text{ nm}}$ was linearly proportional to the dye concentration, whereas the dashed lines in Fig. 3(b) indicate that $\epsilon_{532 \text{ nm}}$ was independent of dye concentration. This is in accordance with the Beer–Lambert law, indicating that dyes did not form absorption complexes in the E49 host.^{20,21}

C. Quantum efficiencies

The results for the quantum efficiencies, η_q , for each dye as a function of concentration, are shown in Fig. 4. In each case, the dye was excited at a wavelength close to the absorption maximum (DCM-doped samples were excited at 475 nm and pyrromethene-doped samples were excited at 514 nm). As the quantum efficiency is the ratio of photons absorbed to photons emitted, the difference in excitation wavelength is not expected to affect the comparison of η_q values between DCM and the pyrromethene dyes. It can be seen that the quantum efficiency of DCM is approximately half of that recorded for the pyrromethene dyes when dispersed in E49. For all dyes the efficiency is found to decrease

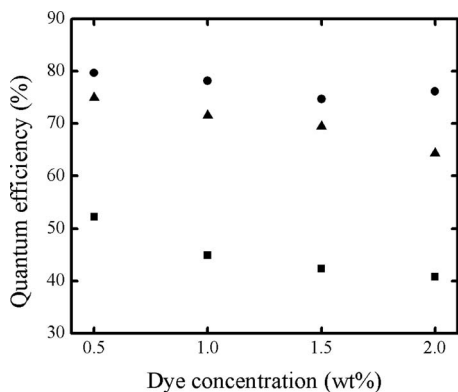


FIG. 4. The quantum efficiency of each dye in the nematic LC host, E49, as a function of concentration by weight. The key for the figure is as follows: DCM (■), PM580 (●), PM597 (▲).

with an increase in concentration, although this effect is far more pronounced for DCM than the pyrromethene dyes. This quantum efficiency represents the probability that the dye molecule will emit a photon upon the absorption of a photon, and it should be noted that the laser threshold is inversely proportional to η_q , whereas the slope efficiency is directly proportional to η_q .²² The high η_q values recorded for the pyrromethene dyes (of the order of 70%–80%) are encouraging for the development of LC lasers, as they indicate that there is little or no nonradiative charge transfer between the pyrromethene dyes and the highly conjugated polar LC host.

D. Fluorescence lifetimes

The fluorescence lifetime, τ , of DCM is shown in Fig. 5, as a function of concentration by weight, for an emission wavelength of 600 nm. These results show that the lifetime is of the order of 2 ns and decreases as the concentration by weight of the dye increases. Both the magnitude and the dependence on concentration are comparable to that observed in the literature for DCM dissolved in methylene chloride.²³ Data are not currently available for the pyrromethene dyes in the LC host but we expect that the lifetimes will also be comparable to those reported in the literature in various solvents. As an example, results for the DCM-dye in ethanol have reported a value of the order of 1.9 ns,²⁴

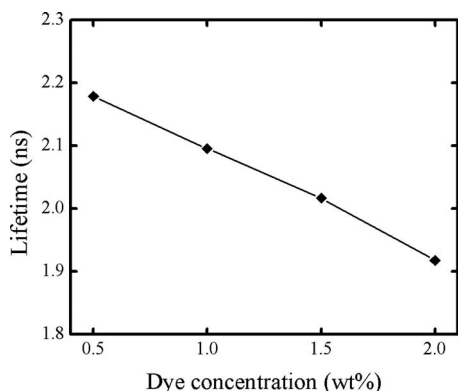


FIG. 5. The time-resolved fluorescence lifetime as a function of concentration by weight for DCM laser dye in the nematic LC host, E49. Data are shown for an emission wavelength of 600 nm (◆). The excitation wavelength was 475 nm.

which is comparable with our results shown here. Fluorescence lifetimes of PM597 and PM580, on the other hand, are reported to be higher in ethanol, being closer to 7 ns.²⁵ Therefore, we expect that the lifetimes of the PM dyes in the LC host will be slightly longer than those already measured for DCM.

E. Optimum laser wavelength

Generally, dye lasers can emit over a relatively broad range of wavelengths. However, the efficiency with which they operate depends on the balance between the gain and losses at the emission wavelength. Consequently, before comparing the threshold and slope efficiency for the different lasers, it was important to determine the wavelength corresponding to maximum efficiency for each dye/E49 combination. This emission wavelength is herein referred to as the optimum wavelength, λ_{opt} .

The optimum wavelength for each dye/E49 combination was determined experimentally for a 1 wt % dye-doped laser sample. The slope efficiency, η_s , is defined as the gradient of the linear region of the input-output curve. This value was measured for a range of different emission wavelengths (in the region of the spontaneous emission peak) for each laser sample. For DCM, the spontaneous emission peaked at $\lambda_{\text{max}}=589$ nm, whereas the spontaneous emission of the pyrromethene dyes peaked at shorter wavelengths (PM580 $\lambda_{\text{max}}=571$ nm and PM597 $\lambda_{\text{max}}=577$ nm).

Coarse tuning of the emission wavelength was achieved by careful control of the amount of chiral dopant in the laser sample. Following this, fine tuning was achieved by translating the cell relative to the pump spot. The alignment layers within the glass cells provided boundary conditions which restricted the helix to an integer number of half turns. Slight variations in thickness across the cells meant that the helix pitch could be slightly stressed with respect to its natural value (either compressed or dilated) at different points in a cell.¹¹ This gave a ≈ 10 nm tuning range in the long band-edge wavelength by varying the cell position.¹⁵ The locations of the optimum wavelengths were assumed to be independent of dye concentration because the shapes of the absorption and spontaneous emission spectra of the dyes were found to be approximately independent of concentration. The λ_{opt} values obtained are summarized as follows: DCM $\lambda_{\text{opt}}=609$ nm, PM580 $\lambda_{\text{opt}}=570$ nm, and PM597 $\lambda_{\text{opt}}=582$ nm. The DCM value of 609 nm is similar to a value of 605 nm for the same DCM concentration (1 wt %) and cell thickness (10 μm) reported elsewhere in the literature.²⁶

F. Laser emission characteristics

Once the optimum wavelength had been determined for each dye/E49 combination, the input-output characteristics were recorded for each type of laser at four different dye concentrations (0.5–2 wt %), see Fig. 6. The data represent the sum of the forward and backward emissions from each laser (measured in the forward direction and doubled). For each sample, the excitation threshold occurred below an input energy of 5 $\mu\text{J}/\text{pulse}$. Above the excitation threshold, the output energies increased linearly with input energy. For

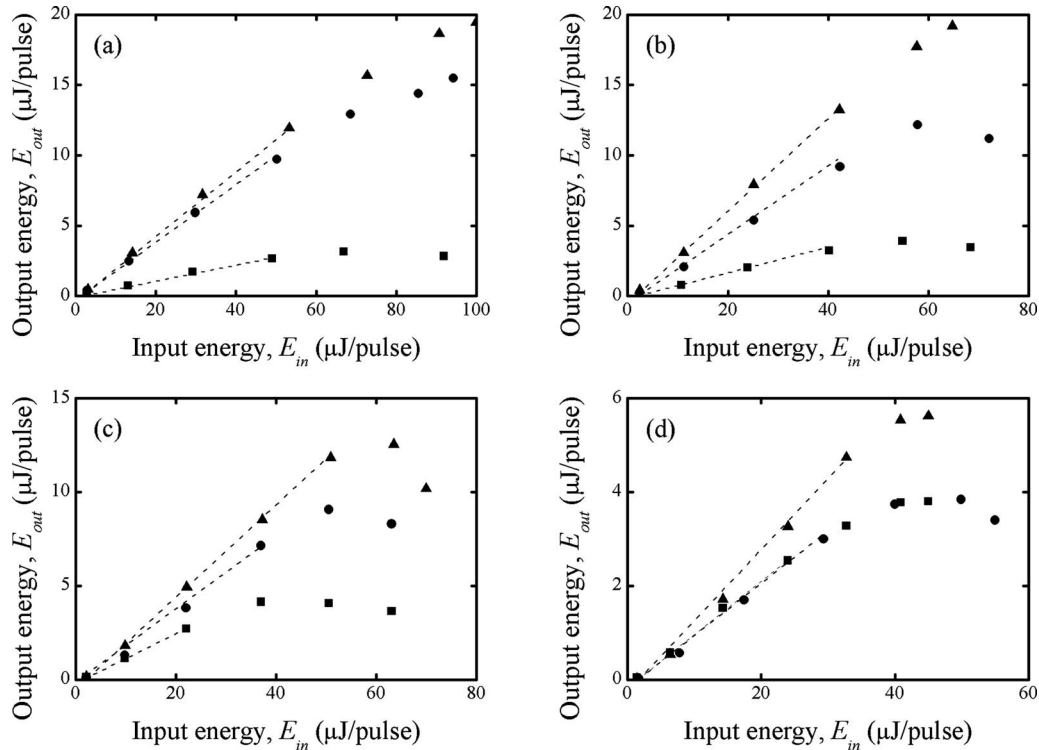


FIG. 6. Input-output characteristics for the PBE lasers. In all cases, the host was E49 doped with BDH1281, the emission wavelength was λ_{opt} , and the cell thickness was $10 \mu\text{m}$. The excitation source was a Nd:YAG laser ($\lambda_{\text{exc}}=532 \text{ nm}$). The output energy of the lasers, E_{out} , was multiplied by a factor of 2 to take into account the emission in the backward direction. The characteristics were graphed by dye concentration: (a) 0.5 wt %, (b) 1.0 wt %, (c) 1.5 wt %, and (d) 2.0 wt % and as a function of dye: DCM (■), PM580 (●), and PM597 (▲). The dashed lines indicate linear regions.

input energies greater than $20 \mu\text{J/pulse}$, the output energies of the laser samples began to reach saturation. However, the saturation point of the 1 wt % PM597 sample was not identified because the forward emission energy was out of the range of the energy meter ($10 \mu\text{J}$).

For the DCM lasers, the maximum output energy recorded was $4 \mu\text{J/pulse}$, corresponding to an excitation energy of $37 \mu\text{J/pulse}$ and a dye concentration of 1.5 wt %. This is in contrast to the PM580 lasers, which exhibited a maximum output energy that was more than a factor of 3 higher ($E_{\text{max}}=15 \mu\text{J/pulse}$). Here the excitation energy was higher ($94 \mu\text{J/pulse}$) and the dye concentration was 0.5 wt %. At such high excitation energies, the DCM lasers had already saturated, and a further increase in excitation energy resulted in a reduction in the emission energy. The maximum output that was recorded for the PM597 lasers was even higher: emission of $19 \mu\text{J/pulse}$ for an input energy of $100 \mu\text{J/pulse}$. However, this does not necessarily represent the absolute maximum output energy of the PM597 laser, as it was limited by the detection range of the energy meter. In accordance with the PM580 laser, the dye concentration for maximum emission was 0.5 wt %.

V. DISCUSSION

To quantify the performance of each laser, we consider the threshold energy, E_{th} , and slope efficiency, η_s , which can be extracted from the input-output curves of Sec. IV F).²⁷ The threshold values were determined from the emission spectra recorded as a function of input energy to increase the sensitivity.²⁸

Figure 7 shows plots of E_{th} as a function of dye concentration for the three laser dyes. For the lowest dye concentration (0.5 wt %), it is shown that the PM580 laser had the lowest threshold ($E_{\text{th}}=110 \text{ nJ/pulse}$), whereas the DCM laser required more energy to generate laser action (E_{th}

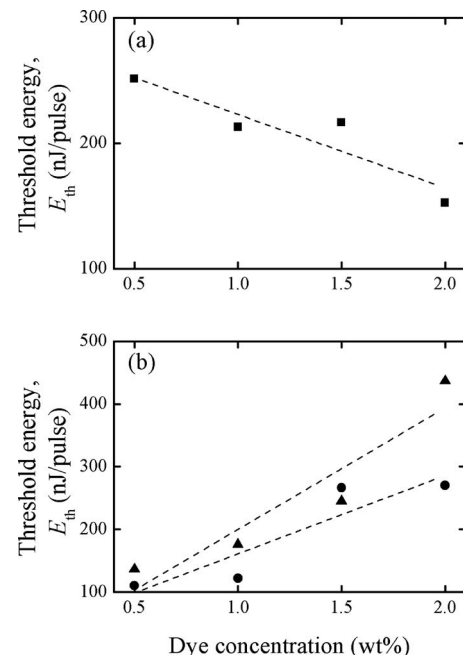


FIG. 7. Threshold energies (E_{th}) of the long-wavelength PBE lasers grouped by dye: (a) DCM (■) threshold as a function of dye concentration. (b) PM580 (●) and PM597 (▲) thresholds as a function of dye concentration. The dashed lines indicate linear fits to the data.

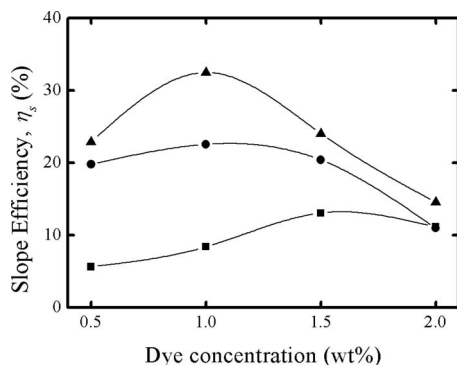


FIG. 8. N*LC laser slope efficiency as a function of dye concentration for DCM (■), PM580 (●), and PM597 (▲).

=251 nJ/pulse). This trend was reversed at the highest dye concentration studied (2 wt %), where the DCM laser sample exhibited the lowest threshold ($E_{th}=152$ nJ/pulse) and the PM580 laser sample had the highest threshold ($E_{th}=270$ nJ/pulse). The threshold energy of each dye was found to depend linearly on dye concentration. However, the DCM laser sample threshold decreased linearly with increasing dye concentration, whereas, in contrast, the thresholds of the PM597 and PM580 laser samples increased with dye concentration.

The slope efficiencies of the N*LC lasers also varied significantly with both dye and concentration, Fig. 8. This is in accordance with previous studies, where optimization of the dye concentration has been shown to increase the emission intensities²⁹⁻³¹ and reduce the threshold energies^{28,30} of N*LC lasers. The most striking feature is that the efficiencies of the PM597 lasers were always higher than those of the two other laser samples, irrespective of dye concentration. Slope efficiencies of the PM597 lasers ranged from 15% to 32%, depending on the concentration of dye. The highest slope efficiency recorded for the PM597 laser is not significantly less than that recorded for the same dye in an isotropic solvent, such as ethanol, but for a transversally pumped dye laser system with mirror spacing approximately four orders of magnitude larger (i.e., ~ 7.5 cm).³²

The DCM laser samples, on the other hand, were always found to have the lowest slope efficiency, ranging from 5% to 13% depending on dye concentration. It is worth noting that the dye concentration corresponding to the maximum slope efficiency was found to be different for each dye. For example, for the PM597 laser samples, the largest slope efficiency ($\eta_s=32\%$) was found to occur at a concentration of 1 wt %, whereas for the DCM laser samples, the efficiency was found to be a maximum at 1.5 wt % with only a modest value of $\eta_s=13\%$. The slope efficiency of the PM580 laser sample also peaked at the same concentration as that of PM597 (1 wt %), although the absolute value was somewhat smaller, $\eta_s=22\%$. Interestingly, for each dye, the concentration exhibiting the highest slope efficiency did not correspond to that exhibiting the lowest threshold energy.

Clearly, the PM597 laser shows the best performance from the point of view of slope efficiency when optically pumped at $\lambda=532$ nm and for a fixed cell thickness of 10 μm , irrespective of the dye concentration. Comparing

directly with DCM, we find that the PM597 dye is better suited for lasing, in this case, in a number of ways. First, the results for the molar extinction coefficient confirm that the absorption is much greater than that of DCM, leading to a greater absorption efficiency. Second, the results for the quantum efficiency reveal that this is significantly higher for PM597 than DCM at all concentrations, indicating that the emission efficiency will in turn be higher. When discussing the factors that affect laser characteristics, Svelto²² used a term known as the pump efficiency, η_p . This describes how well the incident pump energy is transferred to the lasing system and is given by

$$\eta_p = \eta_r \eta_t \eta_a \eta_q, \quad (2)$$

where η_r is the radiative efficiency of the pump source, η_t is the transfer efficiency (the ratio of useful energy entering the amplifying medium to that emitted from the pump source), η_a is the absorption efficiency, and η_q is the quantum efficiency. Svelto showed that laser thresholds are inversely proportional to η_p , whereas the slope efficiencies are directly proportional to η_p . Therefore, all other factors being equal, we would expect materials with high values for absorption efficiency and quantum efficiency to produce lasers with low threshold energies and high slope efficiencies.

The order parameters of the transition dipole moments of both DCM and PM597, S_T , which are believed to affect the stimulated emission rate,^{7,8,11} were calculated from the dye absorption spectra^{33,34} and were found to be comparable for the two dyes ($S_T=0.38 \pm 0.01$ for PM597 and $S_T=0.40 \pm 0.02$ for DCM). The order parameters were found to be independent of dye concentration because the low concentrations used herein did not disrupt the LC matrix. Previous studies^{31,34} have compared the laser emission from DCM-doped N*LC lasers with that from lasers doped with dyes having higher S_T values in the relevant LC host. In both cases, the laser containing the dye with the higher order parameter exhibited greater emission energies at the long-wavelength band edge.

Despite the fact that PM580 is a structural isomer of PM597 and thus has very similar characteristics, the slope efficiency of the corresponding LC laser is found to be somewhat lower for all dye concentrations. The results show that the order parameter and quantum efficiency are slightly higher than those obtained for PM597 when dispersed into the LC; however, the molar extinction is actually slightly lower. Inspection of Fig. 2 shows that the excitation wavelength is located closer to the absorption maximum of PM597 than PM580. A previous report, when optically pumped at 532 nm, has also found the slope efficiency to be higher for the PM597 laser dye, and this was attributed to the closer match between the absorption maximum of PM597 and the excitation wavelength.³²

The results presented in Fig. 7 do show, however, that the thresholds of the PM580 lasers are slightly lower than those observed for the PM597 lasers. This could be due to the fact that the order parameter, S_T , is largest for the PM580 dye [$S_T=0.50 \pm 0.02$ for PM580], given that the molar extinction coefficients are similar. However, at dye concentrations below 1.5 wt%, the thresholds for both the pyr-

romethene dyes are considerably lower than those recorded for the DCM samples, which is in accordance with their higher molar extinction coefficients and quantum efficiencies.

The comparatively low quantum efficiency of DCM dye deserves further consideration. It can be seen from the results that the value of the quantum efficiency is considerably lower for DCM in comparison to the pyrromethene dyes when they are dissolved independently in the same nematic host. In other solvents, reports have shown that the efficiency of DCM can be rather high; for example, in methylene chloride, fluorescence quantum yields as high as 0.9 have been reported.²³ Obviously, this is not the case when the dye is dispersed in a polar LC host such as E49. Ultimately, there are likely to be a number of factors involved; however, perhaps the most likely is charge transfer between the DCM molecule in the excited state and the polar liquid crystalline solvent. This would lead to nonradiative pathways and consequently a reduction in the efficiency. It is known that the dipole moment of DCM in the excited state is significantly higher than that in the ground state, and subsequent intermolecular interactions with the LC may also contribute to lower the quantum efficiency. The pyrromethene dyes, on the other hand, may not exhibit the same interactions and thus their efficiency remains much higher.

Since results are presented for the change in emission behavior with dye concentration, further comment regarding the spatial variation in the dye absorption with respect to the spatial profile of the electric modal field at the long-wavelength PBE is required. The magnitudes of the electric fields of the electromagnetic waves within the sample vary parallel to the helix axis.^{7,35} The intensity of the first allowed mode, corresponding to N*LC PBE laser emission, peaks at the center of the cell.^{7,35} Consequently, the rates of spontaneous and stimulated emission for dye molecules in N*LCs are related to the spatial positions of the dye molecules within the sample. This can be described using a spatially integrated spontaneous emission rate,⁷

$$I_T(\lambda) = \int_0^d p(\lambda, z) e^{-\alpha z} dz, \quad (3)$$

where λ is the pump wavelength, d is the sample thickness, p is the scaled spontaneous emission rate (incorporating both the S_T and space dependencies), z is the distance parallel to the helicoidal axis, and α is the absorption coefficient as defined in Sec. IV B.

Equation (3) cannot be solved analytically but can be investigated numerically by considering that the number of dye molecules excited at the center of the sample (where the probability of emission is greatest) depends on the balance between the amount of pump light reaching the center and the number of molecules available to absorb it. Woon *et al.*⁷ demonstrated a dye-doped N*LC system whose spontaneous emission was more efficient for a low α configuration than a high one. This is because the low α configuration resulted in a better overlap between the excited molecules and the electric modal field of the resonant mode. For the dyes used in this study, the average absorption coefficients at 532 nm

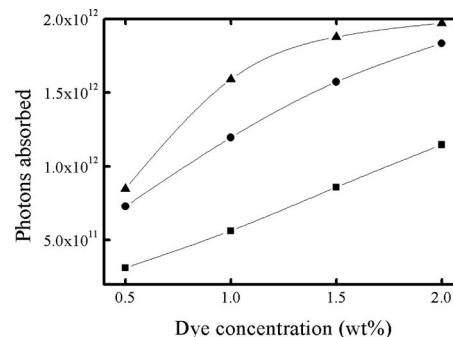


FIG. 9. Number of photons absorbed in the central 1 μm region of a 10 μm cell, as a function of dye: DCM (■), PM580 (●), PM597 (▲), and concentration (10 μJ incident energy).

were used to calculate the number of pump photons absorbed in the central 1 μm region of a 10 μm cell for an incident pump energy of 10 μJ /pulse, see Fig. 9. At 0.5 wt %, and all subsequent dye concentrations, the number of photons absorbed at the center was highest for PM597 and lowest for DCM. In the present case, the spontaneous emission probability (and hence the stimulated emission probability) was found to increase with dye concentration.

In the absence of a complete quantitative model, the exact mechanisms responsible for the dependence of the excitation threshold and slope efficiency on the dye concentration cannot be easily understood, as a number of factors need to be considered in concert. However, it is possible to provide some insight based on the results presented in this work. Herein, it is shown that both the quantum efficiency and the fluorescence lifetime decrease with an increase in the concentration of dye. Generally, the quantum efficiency and fluorescence lifetime of a solution are found to decrease with increasing dye concentration, due to local aggregation or coassociation of the dye molecules.²⁰ This is the most likely explanation for the reduction in the N*LC laser slope efficiencies, and the increase in the thresholds for the pyrromethene lasers, at relatively high dye concentrations, although the dyes did not appear to crystallize macroscopically.

Dye aggregation falls into two categories: that which occurs when all of the molecules are in the ground state (absorption complex formation)^{20,21} and that which occurs when some of the molecules are in the excited state (excimer formation^{20,21} and excited state reactions²⁰). Although absorption complexes can lower the η_q of a solution because they usually emit only weakly, if at all,²⁰ the independence of the molar extinction coefficient from the dye concentration suggests that absorption complexes were not formed, as discussed in Sec. IV B.

Excimer formation, on the other hand, occurs when aggregates form which are only stable in the excited state.^{20,21} Their spontaneous emission is generally redshifted with respect to that of the monomers, and this effect is often used to check for their presence in a system.^{20,21} As discussed earlier (Sec. IV E), the unsaturated spontaneous emission peaks of the achiral dye-doped samples were found to be independent of dye concentration, and no additional emission bands were observed within the wavelength range of the spectrometer.

Therefore, it is unlikely that any reduction in η_q was due to excimer formation. However, excited state reactions can occur when ground and excited state dye molecules collide, transferring energy from the excited to the ground state molecule without emitting a photon. It is not known whether excited state reactions involve the creation of dye dimers for short periods of time (during the energy transfer),²⁰ but if it does they do not emit light.²⁰ In this study, we believe that the reduction in quantum efficiency with increasing dye concentration is due to excited state reactions.

It is important to mention that Cao *et al.*²⁸ also studied the lasing thresholds of DCM-doped N*LC laser samples, using a chiral nematic liquid crystalline host (BLO61, EM industries) diluted with a nematic (E7, EM industries). The range of dye concentrations used here corresponds to their intermediate concentration regime (0.25–2.5 wt % DCM), where they found that E_{th} increased linearly with increasing DCM concentration. The trend was explained in terms of excimer formation, indicated by a redshift in the fluorescence maximum (≈ 7 nm), a reduction in the fluorescence intensity, and a reduction in the fluorescence lifetime with increasing dye concentration. Although the lifetime values measured in the present study are longer than those measured by Cao (e.g., 2.18 ns as opposed to 1.25 ns for 0.5 wt % DCM), we too have observed a decrease in the fluorescence lifetime with increasing DCM concentration (Fig. 5). However, we have not observed a noticeable redshift in the fluorescence maximum and thus believe that, for our samples, the decrease in performance is due to excited state reactions rather than excimer formation.

VI. CONCLUSIONS

The emission characteristics of dye-doped N*LC lasers were studied for the dyes DCM, PM580, and PM597 at different concentrations in the liquid crystalline host. The choice of dye and concentration significantly influenced both the threshold energy and slope efficiency of the resulting laser, when optically pumped at a wavelength of 532 nm. It was found that the pyromethene lasers were considerably better in terms of the threshold and slope efficiency than the DCM lasers. Overall, for the dyes and concentrations used in this study, the best performing dye in terms of slope efficiency was PM597, with values ranging from 15% to 32%. These high efficiencies are comparable with those obtained in the jet stream dye lasers, but where considerably longer cavity lengths are used. On the other hand, PM580 was shown to have the lowest excitation threshold (for a dye concentration of 0.5 wt%). Consequently, for a given optical excitation wavelength, these results show that, by changing the gain medium, the performance of a band-edge LC laser can vary dramatically without any changes to the device architecture. The choice of the combination of gain medium and LC host is of paramount importance in the pursuit of LC laser devices for next-generation applications.

ACKNOWLEDGMENTS

The authors thank Merck NB-C for providing the nematic host (E49) and chiral dopant (BDH1281) and Dr. D. Dukic for the manufacture of a triggering unit for the laser measurements. The authors gratefully acknowledge the Engineering and Physical Sciences Research Council for financial support through the Basic Technology Research Grant Coherent Optical Sources using Micromolecular Ordered Structures (COSMOS) Grant No. EP/D04894X/1.

¹P. J. Collings, *Liquid Crystals: Nature's Delicate Phase of Matter*, 2nd ed. (Princeton University Press, Princeton, 2002).

²E. Yablonovitch, *Phys. Rev. Lett.* **58**, 2059 (1987).

³S. John, *Phys. Rev. Lett.* **58**, 2486 (1987).

⁴V. I. Kopp, B. Fan, H. K. M. Vithana, and A. Z. Genack, *Opt. Lett.* **23**, 1707 (1998).

⁵P. Palffy-Muhoray, W. Cao, M. Moreira, B. Taheri, and A. Munoz, *Philos. Trans. R. Soc. London* **364**, 2747 (2006).

⁶J. R. Willmott, Ph.D. thesis, University of Southampton, 2003.

⁷K. L. Woon, M. O'Neill, G. J. Richards, M. P. Aldred, and S. M. Kelly, *Phys. Rev. E* **71**, 041706 (2005).

⁸S. M. Morris, A. D. Ford, M. N. Pivnenko, O. Hadel, and H. J. Coles, *Phys. Rev. E* **74**, 061709 (2006).

⁹A. D. Ford, S. M. Morris, M. N. Pivnenko, C. Gillespie, and H. J. Coles, *Phys. Rev. E* **76**, 051703 (2007).

¹⁰S. M. Morris, A. D. Ford, M. N. Pivnenko, and H. J. Coles, *J. Appl. Phys.* **97**, 023103 (2005).

¹¹J. Schmidtke and W. Stille, *Eur. Phys. J. B* **31**, 179 (2003).

¹²A. Costela, I. García-Moreno, and R. Sastre, *Phys. Chem. Chem. Phys.* **5**, 4745 (2003).

¹³M. Álvarez, F. Amat-Guerri, A. Costela, I. García-Moreno, C. Gómez, M. Liras, and R. Sastre, *Appl. Phys. B: Lasers Opt.* **80**, 993 (2005).

¹⁴T. G. Pavlopoulos, *Prog. Quantum Electron.* **26**, 193 (2002).

¹⁵S. M. Morris, A. D. Ford, B. J. Broughton, M. N. Pivnenko, and H. J. Coles, *Proc. SPIE* **5741**, 118 (2005).

¹⁶S. M. Morris, A. D. Ford, M. N. Pivnenko, and H. J. Coles, *J. Opt. A, Pure Appl. Opt.* **7**, 215 (2005).

¹⁷I. Dierking, *Textures of Liquid Crystals* (Wiley-VCH, New York, 2003).

¹⁸J. C. de Mello, H. F. Wittmann, and R. H. Friend, *Adv. Mater. (Weinheim, Ger.)* **9**, 230 (1997).

¹⁹S. L. Bondarev, V. N. Knyuksho, V. I. Stepuro, A. P. Stupak, and A. A. Turban, *J. Appl. Spectrosc.* **71**, 194 (2004).

²⁰K. H. Drexhage, in *Dye Lasers*, 3rd ed., edited by F. P. Schäfer (Springer-Verlag, Berlin, 1990).

²¹N. J. Turro, *Modern Molecular Photochemistry* (Benjamin/Cummings, London, 1978).

²²O. Svelto, *Principles of Lasers*, 4th ed. (Plenums, London, 1998).

²³A. M. Taleb, B. T. Chiad, and Z. S. Sadik, *Renewable Energy* **30**, 393 (2005).

²⁴P. R. Hammond, *Opt. Commun.* **29**, 331 (1979).

²⁵E. Yariv, S. Schultheiss, T. Saraidarov, and R. Reisfeld, *Opt. Mater. (Amsterdam, Neth.)* **16**, 29 (2001).

²⁶Y. H. Huang, Y. Zhou, and S. T. Wu, *Appl. Phys. Lett.* **88**, 011107 (2006).

²⁷W. T. Silfvast, *Laser Fundamentals* (Cambridge University Press, Cambridge, 2000).

²⁸W. Cao, P. Palffy-Muhoray, B. Taheri, A. Marino, and G. Abbate, *Mol. Cryst. Liq. Cryst.* **429**, 101 (2005).

²⁹S. K. H. Wei, S. H. Chen, K. Dolgaleva, S. V. Lukishova, and R. W. Boyd, *Appl. Phys. Lett.* **94**, 041111 (2009).

³⁰P. Palffy-Muhoray, A. Munoz, B. Taheri, and R. Twieg, *SID Int. Symp. Digest Tech. Papers* **31**, 1170 (2000).

³¹K. Dolgaleva, S. K. H. Wei, S. G. Lukishova, S. H. Chen, K. Schwert, and R. W. Boyd, *J. Opt. Soc. Am. B* **25**, 1496 (2008).

³²E. Yariv and R. Reisfeld, *Opt. Mater. (Amsterdam, Neth.)* **13**, 49 (1999).

³³B. Bahadur, in *Liquid Crystals: Applications and Uses*, edited by B. Bahadur (World Scientific, London, 1996), Vol. 3.

³⁴K.-C. Shin, F. Araoka, B. Park, Y. Takaniishi, K. Ishikawa, Z. Zhu, T. M. Swager, and H. Takezoe, *Jpn. J. Appl. Phys., Part 1* **43**, 631 (2004).

³⁵V. I. Kopp and A. Z. Genack, *Proc. SPIE* **3623**, 71 (1999).